

Incompressible States of Dirac Fermions in Graphene with Anisotropic Interactions

Vadim M. Apalkov

Department of Physics and Astronomy, Georgia State University, Atlanta, Georgia 30303, USA

Tapash Chakraborty[†]

Department of Physics and Astronomy, University of Manitoba, Winnipeg, Canada R3T 2N2

(Dated: June 26, 2018)

We report on the properties of incompressible states of Dirac fermions in graphene in the presence of anisotropic interactions and a quantizing magnetic field. We introduce the necessary formalism to incorporate the anisotropy in the system. The incompressible state in graphene is found to survive the anisotropy upto a critical value of the anisotropy parameter. The anisotropy also introduces two branches in the collective excitations of the corresponding Laughlin state. It strongly influences the short-range behavior of the pair-correlation functions in the incompressible ground state.

In his quest for a better understanding of the Laughlin state [2], which is widely regarded as the best description of the fractional quantum Hall effect (FQHE) ground states [3] at the primary filling fractions ($\nu = \frac{1}{m}$), Haldane [4] recently demonstrated that the integer and the fractional quantum Hall effects are fundamentally different. In the latter case, he introduced a unimodular (area preserving) spatial metric that characterizes the shape of the correlation functions of the Laughlin state and is obtained by minimizing the correlation energy of the fractional quantum Hall state. This interaction metric is not necessarily congruent to the Galilean metric present in the one-body term of the system Hamiltonian. Such a geometric degree of freedom of the Hamiltonian is totally absent in the integer quantum Hall effect, but its presence helps to explain the success of the many-body state of Laughlin. Subsequent numerical studies [5–7] have elucidated various properties of the incompressible FQHE states in the presence of anisotropic interactions. Anisotropic transport in the FQHE regime is known to exist in higher order filling fractions [8], and has also received some theoretical attention [9]. No such studies have been reported as yet for Dirac fermions in graphene.

Of late, there has been an upsurge of interest on the magnetic field effects on Dirac fermions in graphene [10]. The FQHE states have been investigated by us in monolayer [11] and bilayer [12] graphene. Experimentally, the presence of this effect in monolayer graphene has also been confirmed [13, 14]. Interactions among Dirac fermions play a very important role in graphene, particularly in the quantum Hall regime [15]. Here we investigate the incompressible state of graphene with anisotropic interactions. Our studies indicate that anisotropic interactions brings out several unique features in the system, in particular, in the collective modes and in the pair-correlation functions.

Monolayer graphene in a magnetic field B has a discrete Landau level energy spectrum that is characterized by the Landau level index $n = 0, \pm 1, \pm 2, \dots$ and energy [10, 15] $\varepsilon_n = \hbar\omega_B \text{sgn}(n)\sqrt{|n|}$, where $\omega_B = \sqrt{2}v_F/\ell_0$ and $\ell_0 = \sqrt{\hbar/eB}$ is the magnetic length. Here $\text{sgn}(n) = 0$ if $n = 0$ and $\text{sgn}(n) = \pm 1$ if $n > 0$ and $n < 0$, respectively.

The corresponding wave functions are of the form

$$\Psi_{n,m} = C_n \begin{pmatrix} \text{sgn}(n) i^{|n|-1} \phi_{|n|-1,m} \\ i^{|n|} \phi_{|n|,m} \end{pmatrix}, \quad (1)$$

where $C_{n=0} = 1$ and $C_{n \neq 0} = 1/\sqrt{2}$. The functions $\phi_{n,m}$ are the conventional Landau wavefunctions for a particle obeying the parabolic dispersion relation with the Landau index n and z -component of electron angular momentum m . Such conventional Landau wave functions are characterized by two sets of ladder operators: operator b^\dagger , which raises the Landau index n , and the guiding center ladder operator a^\dagger , which raises the intra-Landau index m . The energy spectrum depends only on n and is highly degenerate with respect to the electron angular momentum m . In Eq. (1) the Landau level wave functions are isotropic, i.e., the electron density depends only on $\rho = \sqrt{x^2 + y^2}$. The basis wave functions (1) are however, not unique. Due to degeneracy of the Landau levels, we can choose any single-particle basis, even anisotropic ones, to describe the properties of the electron system in a strong magnetic field. For the many-electron system with isotropic electron-electron interactions the wave functions (1) are the convenient basis for numerical analysis of the many-electron energy spectrum in a spherical geometry, since the isotropic potential conserve the angular momentum. In the spherical geometry [16], the interaction properties of the many-electron system are described in terms of the Haldane pseudopotentials V_m [16], which are the energies of two electrons with relative angular momentum m . The radius of the sphere, R , is related to integer number $2S$ of magnetic fluxes through the sphere in units of the flux quanta as $R = \sqrt{S}\ell_0$. The single-electron states are characterized by the angular momentum, which is equal to S , and $S_z = -S, \dots, S$. For an isotropic potential, due to the spherical symmetry of the problem the many-particle states are described by the total angular momentum, L , and L_z , while the energy depends only on L . As a result, we can evaluate the energy spectra of the system for a given value of L_z , e.g., $L_z = 0$ [17], which greatly simplifies our analysis of the many-electron system in a given Landau level.

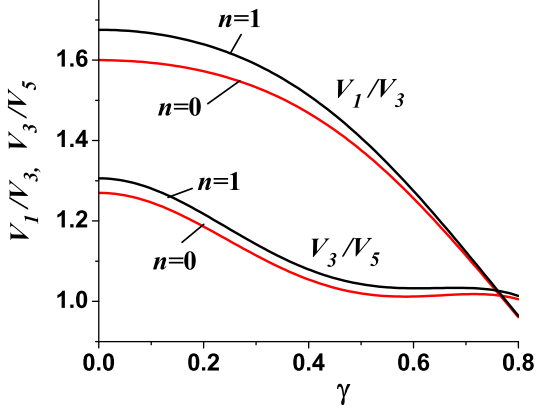


FIG. 1: The ratios of the Haldane's pseudopotentials, V_1/V_3 and V_3/V_5 as a function of γ in two graphene Landau levels $n = 0$ (red lines) and $n = 1$ (black lines).

Here we consider the anisotropic electron-electron interaction potential of the type

$$V(\mathbf{r}_1, \mathbf{r}_2) = \frac{e^2}{\kappa \sqrt{(x_2 - x_1)^2(1 + \gamma) + (y_2 - y_1)^2(1 - \gamma)}}, \quad (2)$$

where $\mathbf{r}_1 = (x_1, y_1)$ and $\mathbf{r}_2 = (x_2, y_2)$ are the coordinates of two electrons, κ is the dielectric constant, and the parameter γ characterizes the anisotropy of the interaction potential with $\gamma = 0$ corresponding to isotropic interaction. We consider the properties of the many-electron system in graphene with fractional filling of the Landau level and with the anisotropic interaction (2). We assume that the interaction does not mix the states of different Landau levels. In this case the interaction potential should be projected on a given Landau level with index n . Although the interaction potential within a given Landau level is anisotropic, we can make it isotropic by introducing a non-uniform scaling transformation of the coordinate system

$$x' = x\sqrt{1 + \gamma}; \quad y' = y\sqrt{1 - \gamma}. \quad (3)$$

The interaction then becomes isotropic $V \propto 1/|\mathbf{r}'_1 - \mathbf{r}'_2|^2$. To take advantage of isotropic potential in the scaled coordinate system, we need to define the angular momentum, which is conserved by the isotropic interaction. Therefore we choose a single-electron basis within a given Landau level, which is initially anisotropic, and define the angular momentum in that anisotropic basis. This procedure was followed in Ref. 5, where the anisotropic Landau level basis states with the non-Euclidean guide center metrics were introduced for the conventional Landau levels. These metrics are characterized by the anisotropy parameter γ . The corresponding guiding center intra-Landau level ladder operators are introduced through the Bogoliubov transformation $a_\gamma = \frac{1}{\sqrt{1 - \gamma^2}}(a + \gamma a^\dagger)$; $a_\gamma^\dagger = \frac{1}{\sqrt{1 - \gamma^2}}(\gamma a + a^\dagger)$. The Landau level basis states of the non-relativistic system

with parabolic dispersion relation are then

$$\phi_{n,m}(\gamma) = \frac{(b^\dagger)^n (a_\gamma^\dagger)^m}{\sqrt{n!m!}} \phi_{0,0}(\gamma), \quad (4)$$

where the state $\phi_{0,0}(\gamma)$ is determined by the condition $a_\gamma \phi_{0,0}(\gamma) = b \phi_{0,0}(\gamma) = 0$. For a given Landau level n the basis function $\phi_{n,m}(\gamma)$ is the linear combination of the isotropic basis functions $\phi_{n,m}(\gamma = 0)$.

In the coordinate representation the zeroth conventional Landau-level function $\phi_{0,0}(\gamma)$ of nonrelativistic electron is given by

$$\phi_{0,0}(\gamma) = \frac{(1 - \gamma^2)^{1/4}}{\sqrt{2\pi}} \exp\left(-\frac{1}{2}\gamma z^2 - \frac{1}{2}|z|^2\right), \quad (5)$$

where $z = x + iy$ is the complex coordinate. Expressing the ladder operators in terms of the complex coordinate, $a = \frac{1}{2}z^* + \partial_z$ and $b = \frac{1}{2}z + \partial_{z^*}$, and using the expression for the anisotropic ladder operators a_γ , we can construct the anisotropic Landau-level basis states from Eq. (4). In graphene, the anisotropic Landau level basis functions are then

$$\Psi_{n,m}(\gamma) = C_n \begin{pmatrix} \text{sgn}(n) i^{|n|-1} \phi_{|n|-1,m}(\gamma) \\ i^{|n|} \phi_{|n|,m}(\gamma) \end{pmatrix}. \quad (6)$$

The angular momentum in this anisotropic basis is m and $L_z(\gamma) = a^\dagger a$. For the many-electron system with anisotropic interaction and anisotropic basis states, the interaction properties are characterized by the Haldane pseudopotentials, V_m , with relative angular momentum $m = m_1 - m_2$. Therefore the interaction energy of two electrons depends only on their relative momentum, but not on the total momentum, $M = m_1 + m_2$. With this property we can study the many-electron system with anisotropic interaction in a spherical geometry, where the total angular momentum is conserved.

We calculate V_m in a planar geometry for the wave functions in Eq. (6) and use these values in the spherical geometry to find the energy spectra of the many-electron system. It is easier to calculate the pseudopotentials V_m for the two-electron system as the interaction energy of two electrons in a state with $M = 0$, and the relative momentum m :

$$V_m = \int d\mathbf{r}_1 d\mathbf{r}_2 |\Phi_m(\gamma, \mathbf{r}_1, \mathbf{r}_2)|^2 V(\mathbf{r}_1, \mathbf{r}_2), \quad (7)$$

where the two-electron state $\Phi_m(\gamma, \mathbf{r}_1, \mathbf{r}_2)$ with relative angular momentum m is

$$\Phi_m(\gamma, \mathbf{r}_1, \mathbf{r}_2) = \frac{(a_{\gamma,1}^\dagger - a_{\gamma,2}^\dagger)^m}{\sqrt{2^m m!}} \phi_{0,0}(\gamma, \mathbf{r}_1) \phi_{0,0}(\gamma, \mathbf{r}_2). \quad (8)$$

Here $a_{\gamma,1}^\dagger$ and $a_{\gamma,2}^\dagger$ are the guiding center ladder operators for electrons 1 and 2, respectively.

In graphene, the FQHE with a large many-particle excitation gap is for $n = 0$ and $n = 1$ Landau levels only,

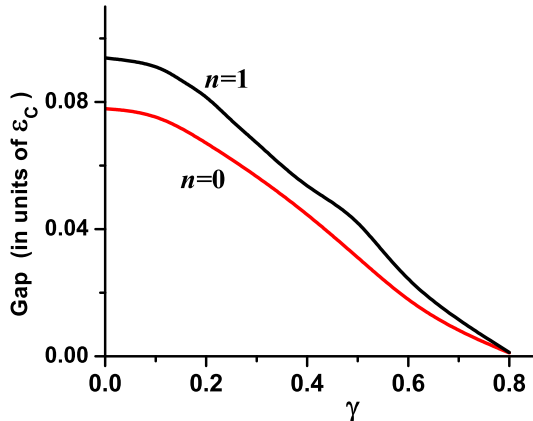


FIG. 2: The $\nu = \frac{1}{3}$ -FQHE gap as a function of γ for the eight-electron system and $n = 0$ (red line) and $n = 1$ (black line). The FQHE gap is calculated in the spherical geometry with flux quanta $2S = 21$.

where the FQHE gap is the largest at $n = 1$ Landau level [11, 15]. Here we consider only these two Landau levels. To characterize the interaction properties of a partially occupied Landau levels, we study the FQHE at a filling factor $\nu = 1/3$. Similar behavior is expected for other filling factors, e.g., $\nu = 1/5, 2/3$.

The wave function of the $n = 0$ graphene Landau level is identical to the $n = 0$ conventional Landau level of nonrelativistic system. Therefore in this case, the interaction properties and the pseudopotentials of graphene and conventional (non-relativistic) systems are identical. The $n = 1$ graphene Landau level is the mixture of $n = 0$ and $n = 1$ conventional Landau wave functions, which introduce specific features into the graphene system.

The magnitude of the FQHE gap depends on how V_m decreases with m . The FQHE with large gap is characterized by large values of the ratios V_1/V_3 and V_3/V_5 . In Fig. 1 we show the ratio of the Haldane pseudopotentials as a function of γ . For all values of γ , the ratios of pseudopotentials are the largest at $n = 1$ Landau level, which suggest that the FQHE state is more stable in $n = 1$ Landau level. With increasing γ , the ratios of the pseudopotentials decrease for both $n = 0$ and $n = 1$ Landau levels, which makes the FQHE less stable at large γ . These results suggest that the FQHE gap decreases with increasing γ and finally collapses for $\gamma \approx 0.8$, when the ratios of pseudopotentials are close to one. To characterize the dependence of the FQHE gap on anisotropy, we evaluate the energy spectra and excitation gap of a finite-size system consisting of $N = 8$ electrons. The $\nu = \frac{1}{3}$ FQHE gap is shown in Fig. 2 as a function of γ . With increasing γ the FQHE gap decreases in both Landau levels, $n = 0$ and $n = 1$. The FQHE gap is larger for $n = 1$. For $\gamma = \gamma_{cr} \approx 0.8$ the FQHE gap disappear and the $\nu = \frac{1}{3}$ state becomes compressible. The critical value γ_{cr} is the same for both Landau levels. This value corresponds to the condition that the pseudopotentials V_1, V_3 ,

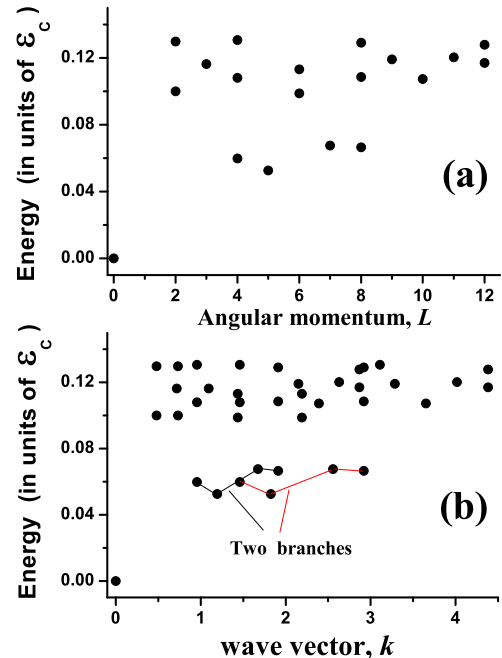


FIG. 3: (a) Energy spectrum of the eight-electron $\nu = \frac{1}{3}$ -FQHE system in the $n = 1$ Landau level. The spectrum is calculated in the spherical geometry with flux quanta $2S = 21$, and $\gamma = 0.4$. (b) The energy spectrum of the eight-electron $\nu = \frac{1}{3}$ -FQHE system for $n = 1$ as a function of the wave vector, k for $\gamma = 0.4$. The results are obtained from the energy spectrum in a spherical geometry and shown in panel (a). The two branches in (b) are shown schematically by black and red lines.

and V_5 become almost the same (Fig. 1). At small values of $\gamma < 0.15$ the FQHE gap shows weak dependence on anisotropy γ .

In spherical geometry, which describes the isotropic system, the energy dispersion is obtained as a function of a total angular momentum, L . Each state has a $(2L + 1)$ degeneracy. The typical energy spectrum is shown in Fig. 2(a) for $\gamma = 0.4$. The energy spectrum has a finite gap and the low energy excited states of the spectrum has well defined single energy branch, showing a roton minimum at finite value of L ($L = 5$ in Fig. 2(a)). In spherical geometry, the excited energy branch is described as a function of the angular momentum $E = E(L)$. Transition to the planar geometry is realized by replacing the angular momentum L by the magnitude of the wave vector $k = L/R$, where R is the radius of the sphere. In this case the energy of the lowest excited states depends on the magnitude of the wave vector but not on its direction, which corresponds to isotropic system.

For anisotropic interactions with anisotropic basis, the energy depends not only on the magnitude of the wave vector k but also on its direction. Such an anisotropic system can be made isotropic under a scaling coordinate transformation determined by Eq. (3). The correspond-

ing transformation in the wave vector space is

$$k'_x = k_x / \sqrt{1 + \gamma}; k'_y = k_y / \sqrt{1 - \gamma}. \quad (9)$$

Each state in the spherical geometry has $(2L + 1)$ degeneracy. In the planar geometry these states correspond to $(2L + 1)$ different directions of wave vector, $\beta_p = 2\pi p / (2L + 1)$, where $p = 1, \dots, 2L + 1$. The corresponding components of the wave vector are $k'_x = \frac{L}{R} \cos \phi_n = \frac{L}{R} \cos \frac{2\pi p}{2L+1}$; $k'_y = \frac{L}{R} \sin \phi_n = \frac{L}{R} \sin \frac{2\pi p}{2L+1}$. These are the components of the wave vector in the scaling coordinate system [Eqs. (9)]. In this case the magnitude of the wave vector depends only on L : $(k'_x)^2 + (k'_y)^2 = (L/R)^2$ and does not depend on the direction.

In the original coordinate system the components of the wave vector are, $k_x = \sqrt{1 + \gamma} k'_x = \sqrt{1 + \gamma} \frac{L}{R} \cos \frac{2\pi p}{2L+1}$; $k_y = \sqrt{1 - \gamma} k'_y = \sqrt{1 - \gamma} \frac{L}{R} \sin \frac{2\pi p}{2L+1}$, and the magnitude of the wave vector is $k_p = \sqrt{k_x^2 + k_y^2} = \frac{L}{R} \sqrt{1 + \gamma \cos \frac{4\pi p}{2L+1}}$. The magnitude of the wave vector now depends on the direction. In the original coordinate system, each energy level $E(L)$ with a given angular momentum L produces $(2L + 1)$ states with different wave vectors k_p . In the thermodynamic limit ($R \rightarrow \infty$), these wave vectors accumulate in two directions, corresponding to the points of large density, which is proportional to $1/(dk_p/dp)$. This condition determines two values of the wave vector $k_1 = \frac{L}{R} \sqrt{1 + \gamma}$ and $k_2 = \frac{L}{R} \sqrt{1 - \gamma}$, which results in two branches in the low-energy dispersion relation of graphene. These branches are shown in Fig. 3(b) for $\gamma = 0.4$. The energy dispersion shown in Fig. 3(b) is recalculated from the energy spectrum obtained in the spherical geometry and shown in Fig. 3(a). Splitting of the magneto-roton mode was first observed experimentally for conventional semiconductor system [18] and was explained as a result of intrinsic anisotropy in the system [19]. Experimental confirmation of such splitting in graphene would be very an important step forward.

Properties of the incompressible state can also be characterized by the pair-correlation function,

$$g(\mathbf{r}) = \int \dots \int d\mathbf{r}_3 \dots d\mathbf{r}_N |\Phi_0(\gamma, 0, \mathbf{r}, \mathbf{r}_3, \dots, \mathbf{r}_N)|^2, \quad (10)$$

where $\Phi_0(\gamma, \mathbf{r}_1, \mathbf{r}_2, \mathbf{r}_3, \dots, \mathbf{r}_N)$ is the N -particle wave function of the incompressible ground state. The ground state of the many-particle system is initially calculated in the spherical geometry for a special single-particle basis [17], where the states of such basis are characterized by L_z . Then each basis state of the spherical geometry, in the expression for the ground state of the many-electron system is replaced by the corresponding anisotropic state of the planar geometry with the same z component of the angular momentum, $m = L_z$. The pair-correlation function in planar geometry is calculated in this way and are shown for different values of γ in Fig. 4.

For $\gamma = 0$, the pair-correlation function $g(\mathbf{r})$ is isotropic and depends only on the magnitude of \mathbf{r} . For $n = 0$

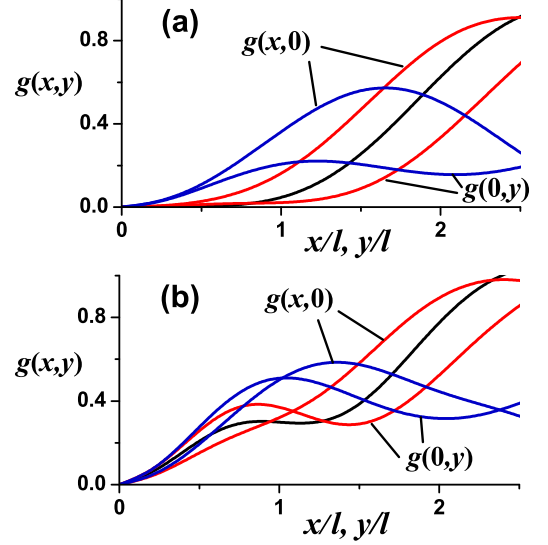


FIG. 4: The pair-correlation function $g(x, y)$ for the eight-electron $\nu = \frac{1}{3}$ -FQHE system in the incompressible ground state for different anisotropy parameters: $\gamma = 0$ (black line), $\gamma = 0.2$ (red line), and $\gamma = 0.6$ (blue line). The results are for the spherical geometry with the flux quanta $2S = 21$. We considered two Landau levels with indices (a) $n = 0$ and (b) $n = 1$. For $\gamma \neq 0$, the correlation function is anisotropic. For an anisotropic system, the correlation functions are shown along the x ($y = 0$) and y ($x = 0$) directions.

(Fig. 4a), the incompressible state of the system is described by the Laughlin state, which results in $g(r) \propto r^6$ for small r . With increasing anisotropy, the correlation function becomes anisotropic and show quadratic dependence on r , which is correlated with suppression of the FQHE gap. Even for $\gamma = 0.2$, when the FQHE gap is still large, the system shows a strong deviation of the pair-correlation function from the isotropic case. With increasing anisotropy the pair-correlation function shows local maxima for some finite values of r , which suggests a transition to compressible state with crystalline structure [7]. For $n = 1$ (Fig. 4b), due to the presence of both $n = 0$ and $n = 1$ conventional Landau wave functions in a single-electron basis [Eq. (6)], the pair-correlation function has a quadratic dependence on r , even in the isotropic case. With increasing anisotropy, just as for $n = 0$, the pair correlation function develops additional local maximum for finite values of r . The anisotropy of the pair-correlation function in $n = 1$ is much weaker than that for $n = 0$, which suggests a more stable FQHE in the $n = 1$ Landau level. This is consistent with the behavior of FQHE gap in different Landau levels [Fig. 3].

The work has been supported by the Canada Research Chairs Program of the Government of Canada.

-
- [†] Electronic address: tapash@physics.umanitoba.ca
- [2] R.B. Laughlin, Phys. Rev. Lett. **50**, 1395 (1983).
- [3] T. Chakraborty and P. Pietiläinen, *The Quantum Hall Effects* (Springer, New York 1995) 2nd. edition.
- [4] F.D.M. Haldane, Phys. Rev. Lett. **107**, 116801 (2011).
- [5] R.-Z. Qiu, F.D.M. Haldane, X. Wan, K. Yang, and S. Yi, Phys. Rev. B **85**, 115308 (2012).
- [6] B. Yang, Z. Papic, E.H. Rezayi, R.N. Bhatt, and F.D.M. Haldane, Phys. Rev. B **85**, 165318 (2012).
- [7] H. Wang, R. Narayanan, X. Wan, and F.C. Zhang, Phys. Rev. B **86**, 035122 (2012).
- [8] R.R. Du, W. Pan, H.L. Stormer, D.C. Tsui, L.N. Pfeiffer, K.W. Baldwin, and K.W. West, Physica E **6**, 36 (2000); W. Pan, R.R. Du, H.L. Stormer, D.C. Tsui, L.N. Pfeiffer, K.W. Baldwin, and K.W. West, Phys. Rev. Lett. **82**, 820 (1999); M.P. Lilly, K.B. Cooper, J.P. Eisenstein, L.N. Pfeiffer, and K.W. West, Phys. Rev. Lett. **82**, 394 (1999).
- [9] K. Musaelian and R. Joynt, J. Phys.: Condens. Matter **8** L105 (1996); O. Ciftja and C. Wexler, Phys. Rev. B **65**, 045306 (2001); M. Mulligan, C. Nayak, and S. Kachru, Phys. Rev. B **82**, 085102 (2010).
- [10] D.S.L. Abergel, V. Apalkov, J. Berashevich, K. Ziegler, and T. Chakraborty, Adv. Phys. **59**, 261 (2010).
- [11] V.M. Apalkov and T. Chakraborty, Phys. Rev. Lett. **97**, 126801 (2006).
- [12] V.M. Apalkov and T. Chakraborty, Phys. Rev. Lett. **105**, 036801 (2010); Phys. Rev. Lett. **107**, 186803 (2011).
- [13] D.A. Abanin, I. Skachko, X. Du, E.Y. Andrei, and L.S. Levitov, Phys. Rev. B **81**, 115410 (2010).
- [14] F. Ghahari, Y. Zhao, P. Cadden-Zimansky, K. Bolotin, and P. Kim, Phys. Rev. Lett. **106**, 046801 (2011).
- [15] T. Chakraborty and V.M. Apalkov, to be published in Solid State Communications (special issue on graphene) (2013).
- [16] F.D.M. Haldane, Phys. Rev. Lett. **51**, 605 (1983).
- [17] G. Fano, F. Ortolani, and E. Colombo, Phys. Rev. B **34**, 2670 (1986).
- [18] C.F. Hirjibehedin, Irene Dujovne, A. Pinczuk, B.S. Dennis, L.N. Pfeiffer, K.W. West, Phys. Rev. Lett. **95**, 066803 (2005).
- [19] I.V. Tokatly and G. Vignale, Phys. Rev. Lett. **98**, 026805 (2007).